

See discussions, stats, and author profiles for this publication at: <https://www.researchgate.net/publication/8333194>

Experimental indication for the existence of multiple Trp rotamers in von Willebrand Factor A3 domain

ARTICLE in PROTEINS STRUCTURE FUNCTION AND BIOINFORMATICS · NOVEMBER 2004

Impact Factor: 2.63 · DOI: 10.1002/prot.20227 · Source: PubMed

CITATIONS

10

READS

15

7 AUTHORS, INCLUDING:



[Yves Engelborghs](#)

University of Leuven

235 PUBLICATIONS 6,535 CITATIONS

[SEE PROFILE](#)



[Hans Deckmyn](#)

University of Leuven

282 PUBLICATIONS 6,413 CITATIONS

[SEE PROFILE](#)



[Karen Vanhoorelbeke](#)

University of Leuven

113 PUBLICATIONS 2,353 CITATIONS

[SEE PROFILE](#)



[Marc De Maeyer](#)

University of Leuven

119 PUBLICATIONS 3,244 CITATIONS

[SEE PROFILE](#)

Experimental Indication for the Existence of Multiple Trp Rotamers in von Willebrand Factor A3 Domain

Mario Hellings,¹ Yves Engelborghs,¹ Hans Deckmyn,² Karen Vanhoorelbeke,² Marion E. Schiphorst,³ Jan Willem N. Akkerman,³ and Marc De Maeyer^{4*}

¹Laboratory of Biomolecular Dynamics, Katholieke Universiteit Leuven, Leuven, Belgium

²Laboratory for Thrombosis Research, IRC, Kortrijk, Belgium

³Laboratory for Thrombosis and Haemostasis, Department of Haematology, University Medical Center, Utrecht, The Netherlands

⁴Laboratory of Biomolecular Modelling, Katholieke Universiteit Leuven, Leuven, Belgium

ABSTRACT The first step in both normal haemostasis and arterial thrombosis is the interaction between collagen, von Willebrand factor (vWF), and glycoprotein Ib. The A3 domain of vWF forms the principal binding site for collagen type I and type III. Inhibition of the vWF-collagen interaction by an anti-human vWF monoclonal antibody (MoAb) 82D6A3 can be a potential way to prevent arterial thrombosis. Identification of the epitope of MoAb 82D6A3 showed recently that the consensus sequence SPWR obtained by phage display could adopt the conformation of the discontinuous epitope. Modelling showed that Trp982 in the vWF had to obtain a more solvent accessible conformation. We performed a detailed fluorescence study of Trp982 in the vWF A3. Using the method described by Hellings et al. (Biophys J 2003;85:1894–1902), we were able to identify two different low-energy Trp982 rotamers and to link them with their experimentally derived fluorescence lifetimes. Fluorescence anisotropy showed no interconversion in the nanosecond time-scale between the two different rotameric states. With these experiments, we gather strong indications for the existence of an exposed rotamer conformation and a rotamer that corresponds to the one observed in the X-ray structure. These results strongly support the modeling work (Vanhoorelbeke et al., J Biol Chem 2003;278:37815–37821). Proteins 2004;57:596–601. © 2004 Wiley-Liss, Inc.

Key words: von Willebrand factor; fluorescence lifetime; fluorescence anisotropy; tryptophan rotamers; thrombosis

INTRODUCTION

Platelet adhesion to vascular subendothelium or to other intravascular surfaces is the initial event in both normal haemostasis and arterial thrombosis. The von Willebrand Factor (vWF) plays an essential role in the initial adhesion of platelets to damaged blood vessels.¹ This factor mediates platelet adhesion both to the damaged vessel wall, primarily through collagen, and to glycoprotein Ib located on the platelet membrane. The vWF A3 domain (922–1,111), a 24-kDa domain, forms the main collagen type I and type III binding site.^{1,2} It consists of a

central six-stranded β -sheet surrounded by seven α -helices and contains a single tryptophan residue at position 982.¹ Specific blockade of the vWF-collagen interaction could be an antithrombotic strategy as described by Wu et al.³ These authors used an anti-human vWF monoclonal antibody (MoAb) 82D6A3, which by binding to the vWF A3 domain inhibits the vWF-collagen interaction. Their results indicated the importance of the vWF-collagen interaction in vivo in thrombosis under high shear conditions.

In a recent study, the epitope of the MoAb 82D6A3 was identified using phage display of a randomized cyclic octa and linear 15-mer peptides together with site-directed mutagenesis of the vWF A3 domain.⁴ The phage consensus sequence SPWR was identified and the structure CMTSP-WRC was modeled and manually fitted onto the vWF A3 domain.⁴ The authors obtained an acceptable superposition under the condition that Trp982 in the vWF was rotated into the solvent. This indicated that the consensus SPWR-sequence could mimic the discontinuous epitope, provided the Trp obtains a more solvent-accessible conformation as compared to the crystal structure.

In this article, we provide a strong experimental indication that the proposed modeled position of Trp982 is indeed possible. Hellings et al.⁵ developed a method to identify tryptophan rotamers in a single-Trp protein and to correlate them with their respective fluorescence lifetimes. Therefore, we performed a detailed fluorescence study of Trp982 in the vWF A3 domain. We also determined the possible low-energy conformations of this Trp with the dead-end method as described by Hellings et al.⁵ This method allowed us to link the different rotamers with the experimentally derived fluorescence data.⁵ The absence of fast interconversion between the rotamers was checked with fluorescence anisotropy measurements.

Grant sponsor: Fund for Scientific Research of the Flanders; Grant numbers: G.0092.01 and 1.5.159.03; Grant sponsor: Inter University Attraction Pole; Grant number: UAP/P5/33.

*Correspondence to: Prof. Dr. Marc De Maeyer, Katholieke Universiteit Leuven, Laboratory of Biomolecular Modelling, Celestijnenlaan 200D, 3001 Leuven, Belgium.
E-mail: Marc.DeMaeyer@fys.kuleuven.ac.be

Received 13 January 2004; Accepted 30 April 2004

Published online 12 July 2004 in Wiley InterScience (www.interscience.wiley.com). DOI: 10.1002/prot.20227

MATERIALS AND METHODS

Materials

The vWF A3 domain was obtained as described previously.¹ Acrylamide and N-acetyltryptophanamide (NATA) were purchased from Sigma Chemical Company (St Louis, MO). All other chemicals were of analytical grade. Distilled and deionized water (ddH₂O) was used throughout the experiments. The buffer solution used for the fluorescence measurements contained 25 mM Tris pH 8.2, 2.5 mM CaCl₂, and 50 mM NaCl. All solutions were filtered through a 0.22-μm filter (Millipore Co., Bedford, MA) and were spectroscopically pure.

Multifrequency Phase Fluorometry

Fluorescence lifetimes were measured using automatic multifrequency phase fluorometry between 1.6 MHz and 1 GHz as described previously.⁶ NATA in ddH₂O with a fluorescence lifetime of 3.059 ns (at 22°C) was used as reference. Data analysis was performed using a nonlinear least-squares algorithm.⁷ Measurements performed at different emission wavelengths (320–380 nm) were analyzed simultaneously with global analysis (Globals Unlimited™) to improve the recovery of lifetimes and amplitude fractions.⁸ The data were fitted using the modified Levenberg-Marquardt algorithm assuming that the fluorescence lifetimes are independent of the wavelength.⁹

Determination of the Radiative Rate Constant

Quantum yields were determined relative to tryptophan in water according to the method of Parker and Rees¹⁰:

$$Q_{\text{Prot}} = \left[\left(\int I_{\text{Prot}} A_{\text{Trp}} \right) / \left(\int I_{\text{Trp}} A_{\text{Prot}} \right) \right] \cdot Q_{\text{Trp}} \quad (1)$$

where $\int I$ is the integrated intensity over the wavelength region 300–450 nm. A is the absorbance at 295 nm, and the quantum yield Q_{Trp} for tryptophan in water is taken as 0.14.¹¹

The average radiative rate constant is calculated by dividing the quantum yield by a wavelength independent amplitude-average lifetime¹²:

$$\langle k_r \rangle = Q / \sum \tau_i \alpha_i \quad (2)$$

with $\sum \tau_i \alpha_i$ the average lifetime, α_i is a wavelength-independent amplitude fraction and is defined as¹²:

$$\alpha_i = \left(\int I_{0i}(\lambda) d\lambda \right) / \left(\int I_0(\lambda) d\lambda \right) \quad (3)$$

The fluorescence intensity at time zero $I_0(\lambda)$ associated with each lifetime is integrated over the wavelength region 300–450 nm and then normalized.

Time-Resolved Anisotropy

Time-resolved anisotropy measurements were obtained from the frequency-dependent phase angle difference between the parallel and perpendicular components of the modulated fluorescence emission. These values are fitted

to the frequency transform of a multi-exponential anisotropy decay law.¹³

$$r(t) = r_0 \sum_i g_i e^{-t/\phi_i} \quad (4)$$

where r_0 is the anisotropy at time zero, and g_i and ϕ_i are the pre-exponential factor and the rotational correlation time for component i ($\sum g_i = 1$), respectively. The analysis was performed assuming that each fluorescing species with lifetime τ_i has the same anisotropy function.¹⁴ No indication for associative decay was found.

Fluorescence Quenching

The quenching of Trp982 in the vWF A3 domain (10 μM) with increasing amounts of quencher was performed by adding aliquots of a freshly prepared 1 M acrylamide stock solution to the cuvette, after which the changes in the fluorescence lifetimes (τ_i) and corresponding amplitude fractions (α_i) were monitored. The dependence of the reciprocal fluorescence intensity on the quencher concentration $[Q]$ was fitted by the classical Stern-Volmer equation¹⁵ and used to calculate k_q .

Determination of Tryptophan Rotamers

To determine the possible conformations of Trp982 in the vWF A3 domain, we used the dead-end elimination method.¹⁶ The identification of the rotamer clusters occurs as previously described by Hellings et al.⁵ A full-hydrogen model and energy-minimized X-ray structure (PDBID: 1ATZ) was used as the starting structure. The rotamer library we used was an enhanced version of the libraries of De Maeyer et al.¹⁷ The DEE algorithm has been implemented in the Brugel package.¹⁸ All calculations were performed on a single processor of a four processor Silicon Graphics Origin 2100 (R10000, 250 MHz).

Solvent-Accessible Area Calculation

The solvent-accessible surface areas were calculated with the “Survoll” option in the Brugel software package,¹⁸ using a probe sphere with a standard radius of 1.4 Å.¹⁹

RESULTS

Rotamer Clusters of Tryptophan

Using the Dead-End method, two rotamer clusters were found for Trp982 of the vWF A3 domain as shown in Figure 1(B). The first and second rotamer cluster have an average calculated accessible surface area (ASA) of respectively 1.68 and 18.52% of their maximal possible accessibility (264 Å²). For each of the two observed clusters, the mean distance between the indole Cε3 atom and the C atom of the peptide carbonyl is calculated. These mean values are 5.3 ± 0.11 Å and 4.6 ± 0.06 Å for the first and second rotamer cluster, respectively.

Fluorescence Lifetimes and Quenching With Acrylamide

The fluorescence decay of Trp982 in the vWF A3 domain was measured at emission wavelengths ranging from 320 to 380 nm in 10-nm intervals. The decay curves were

TABLE I. Fluorescence Lifetimes (τ) and Amplitude Fractions (α) of Trp982 in the vWF A3 Domain[†]

α_1	τ_1 (ns)	α_2	τ_2 (ns)	χ^2	Acrylamide (M)
0.14 ± 0.050	2.08 ± 0.24	0.86 ± 0.020	6.26 ± 0.15	1.30	0.00
0.11 ± 0.013	1.69 ± 0.17	0.89 ± 0.020	6.16 ± 0.10	1.10	0.05
0.13 ± 0.014	1.67 ± 0.13	0.87 ± 0.012	5.84 ± 0.10	1.11	0.10
0.13 ± 0.015	1.35 ± 0.14	0.87 ± 0.009	5.21 ± 0.09	1.42	0.20
0.14 ± 0.030	1.20 ± 0.15	0.86 ± 0.040	4.82 ± 0.11	1.20	0.30
0.16 ± 0.040	1.08 ± 0.14	0.84 ± 0.050	4.47 ± 0.14	1.80	0.40

[†]The quenching of Trp982 in the vWF A3 domain (10 μ M) with increasing amounts of acrylamide. The measurements were performed at 20°C. χ^2 is the value that defines the correctness of the fit.

analyzed by single-curve analysis of the data at each wavelength and global analysis of data for seven emission wavelengths. The sum of two exponential terms was adequate to fit the data and yielded lifetime components of 2.08 ns (τ_1) and a longer one of 6.26 ns (τ_2). Table I shows the results of the global fit for Trp982 of the vWF A3 domain.

Hellings et al.⁵ developed a method to link the different tryptophan rotamers with their respective fluorescence lifetimes on basis of the relation between the accessible surface area and the bimolecular quenching constant k_q . Therefore, we monitored the time-resolved fluorescence quenching by acrylamide. The effect of adding acrylamide was not the same on the different lifetime components. Table I shows the results of quenching the vWF A3 domain with acrylamide. The two rate constants (reciprocal lifetimes) show a linear dependence for the acrylamide concentration. The values for the bimolecular quenching constant k_q are $1.075 \pm 0.07 \text{ M}^{-1} \text{ ns}^{-1}$ and $0.168 \pm 0.008 \text{ M}^{-1} \text{ ns}^{-1}$ for τ_1 and τ_2 , respectively. The value of k_q for the short-lifetime component is sixfold larger than that of the longer one, indicating that the short-lifetime component is associated with a more solvent accessible conformer.

Fluorescence Anisotropy

Time-resolved fluorescence anisotropy measurements were performed on Trp982 of the vWF A3 domain to gain information about the mobility of the Trp residue. The best fit was obtained with a single exponential decay giving a rotational correlation time (ϕ) of $13.5 \pm 1.5 \text{ ns}$ and a r_0 value of 0.22 ± 0.015 . For a spherical protein in water, with a relative molecular mass equal to 24 kDa and a hydration of 0.2g H₂O per g protein,¹⁵ a rotational correlation time of 11.06 ns can be obtained using the Stokes-Einstein equation ($\phi = \eta V/kT$, where η is the viscosity of water and V is the hydrated volume). The measured value is comparable to the calculated value and can be attributed to the global rotation of the vWF A3 domain. These measurements indicate that rotamer interconversion, if at all possible, is a lot slower than the nanosecond timescale.

DISCUSSION

The existence of rotamers as an explanation for the different lifetimes of tryptophan was first proposed by Szabo and Rayner.²⁰ Using the Dead-End method, we find two rotamer clusters, one with an average ASA of 1.68%

(4.44 Å²) and another with an average ASA of 18.52% (48.89 Å²). The quenching experiments with acrylamide yield two bimolecular quenching constants indicating that the rotamer with the short lifetime is more solvent-accessible. According to these results, the cluster with the highest ASA should therefore be linked with the short fluorescence lifetime of tryptophan. In this rotamer assignment, we also observe that the shortest lifetime correlates with the shortest distance between Ce3 and the peptide carbonyl C atom, as found for many other Trp rotamers by Hellings et al.⁵

All these observations link rotamer cluster 1 and 2, respectively, with the long-lifetime component (τ_2) and short-lifetime component (τ_1) and provide a strong experimental indication for the existence of the two rotamer clusters. Rotamer cluster 1 corresponds to the conformation of Trp982 found in the X-ray structure. Rotamer cluster 2 corresponds to the more solvent exposed conformation that coincides with the proposed modeled conformation of Trp982, which overlaps with the one of the cyclic peptide CMTSPWRC [Fig. 1(C)]. The energy minimum of each cluster ($\chi_1 = -70^\circ$; $\chi_2 = 130^\circ$) and ($\chi_1 = -10^\circ$; $\chi_2 = -120^\circ$) for cluster 1 and 2, respectively, is shown in Figure 1(A). The results of the modeling of the cyclic peptide⁴ are shown in Figure 1(C). To compare these rotamer clusters with experimentally observed X-ray rotamers, we plotted the chi-angles of all Trp residues from proteins with a resolution better than 3Å and containing a maximum of 3 Trp residues (Fig. 2). This plot shows that both rotamers are populated in the Brookhaven Protein Databank, although less for the alternative rotamer cluster 2. We demonstrated that an additional Trp rotamer different from the one observed in the X-ray structure is compatible with the proposed modeling work.⁴ These results can simplify a docking study of the vWF A3 domain with the MoAb 82D6A3.

CONCLUSIONS

We performed a detailed fluorescence study of Trp982 in the vWF A3 domain and determined the low-energy tryptophan conformations. Using the method described by Hellings et al.,⁵ we were able to identify two different rotamers and to link them with their experimentally derived fluorescence lifetimes. Fluorescence anisotropy showed no interconversion in the nanosecond timescale between the two different rotameric states. With these experiments, we

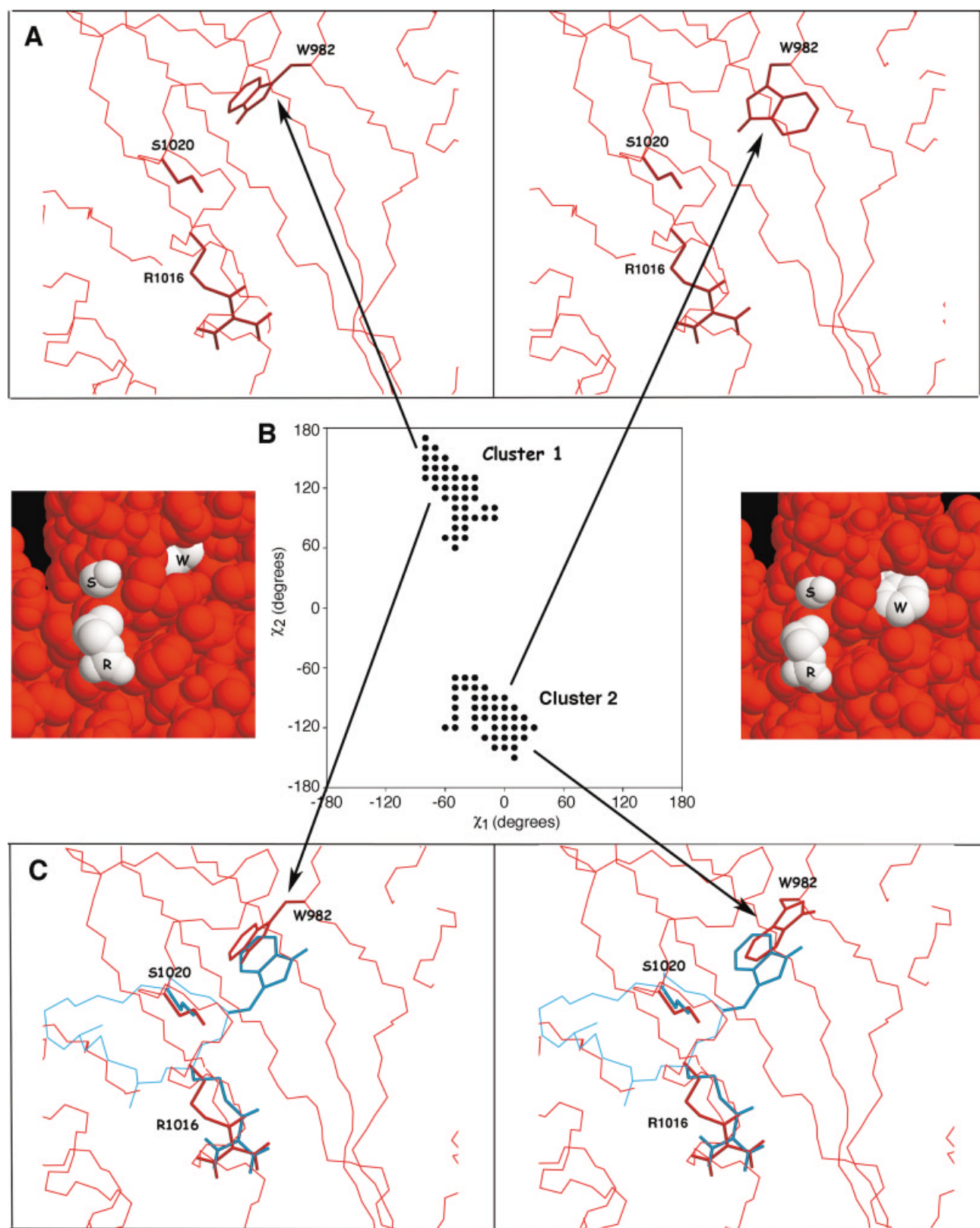


Fig. 1. Rotamer representation of Trp982 in the von Willebrand Factor A3 domain. Using the method described by Hellings et al.,⁵ two rotamer clusters are found for Trp982 of the vWF A3 domain (**B**). In all the wireframe panels, the crystal structure is shown in red and the peptide in blue. The energy minimum of each cluster, ($\chi_1 = -70^\circ$; $\chi_2 = 130^\circ$) and ($\chi_1 = -10^\circ$; $\chi_2 = -120^\circ$) for cluster 1 and 2, respectively, is shown in **A**. Rotamer cluster 1 (**A**, left) corresponds to the conformation of Trp982 found in the X-ray structure (**C**, left). Rotamer cluster 2 (**A**, right) represents the more solvent exposed modeled Trp982 conformation overlapping with the modeled cyclic CMTSPWRC peptide (**C**, right). CPK models, for the buried (left) and exposed Trp982 (right) are shown, highlighting the degree of solvent exposure for each rotamer cluster (vWF is shown in red; Trp982, R1016, and S1020 are shown in white).

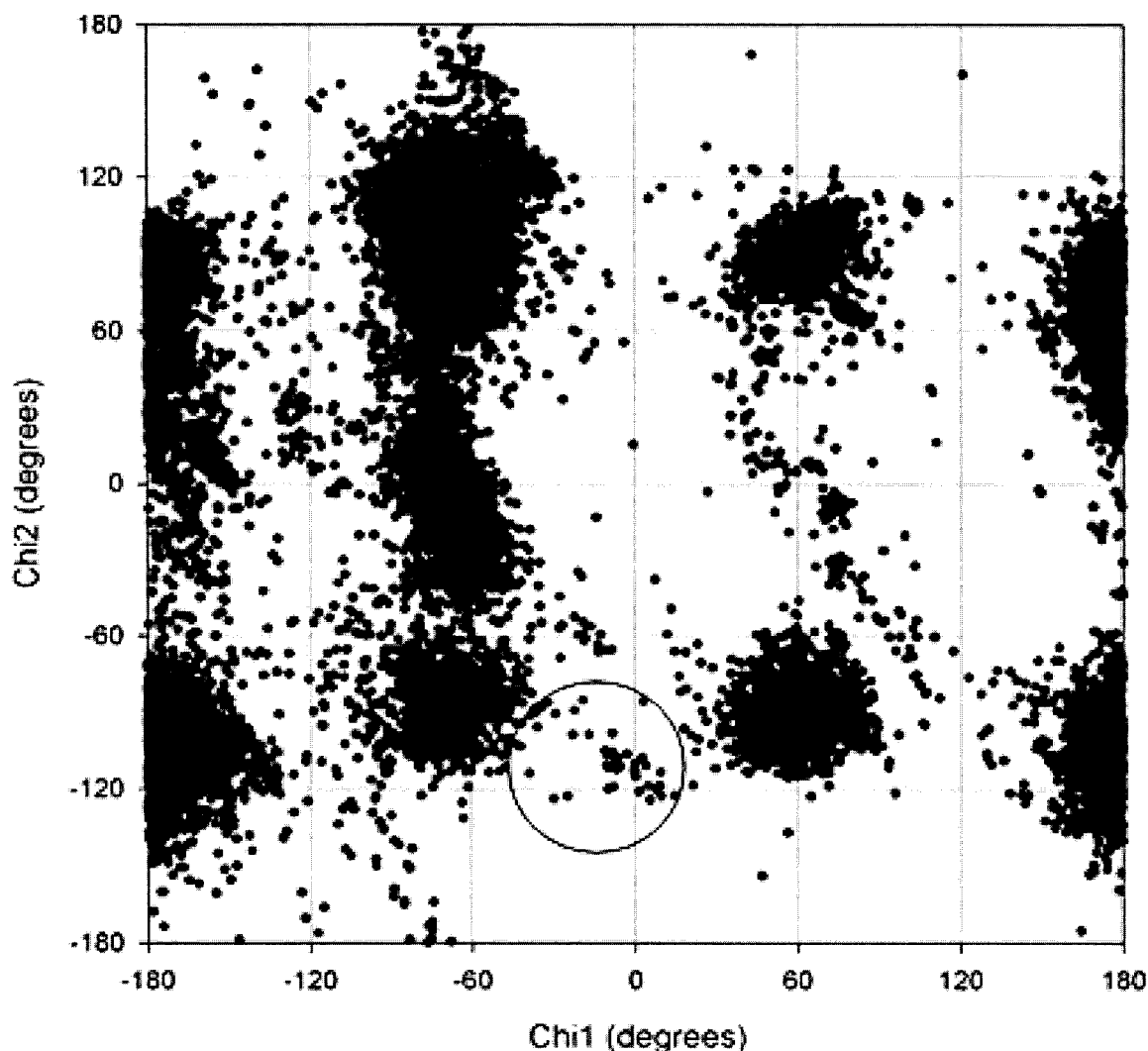


Fig. 2. χ_1 , χ_2 plot of protein X-ray structures with a resolution better than 3 Å and containing maximum 3 Trp residues. The circled region indicates the position of the alternative rotamer cluster we observed.

gather strong indications for the existence of an exposed rotamer conformation and a rotamer that corresponds to the one observed in the X-ray structure. The more solvent exposed conformation coincides with the proposed modeled conformation of Trp982, which overlaps with the one of the cyclic peptide CMTSPWRC.⁴ The larger accessibility of the side chain atoms of the more solvent exposed conformation of Trp982 can improve binding of the MoAb 82D6A3. Future docking experiments can provide additional confirmation for the existence and necessity of the more exposed rotamer of Trp982.

REFERENCES

1. Huizinga EG, Van der Plas MR, Kroon J, Sixma JJ, Gros P. Crystal structure of the A3 domain of human von Willebrand factor: implications for collagen binding. *Structure* 1997;5:1147–1156.
2. Romijn RA, Westein E, Bouma B, Schiphorst ME, Sixma JJ, Lenting PJ, Huizinga EG. Mapping the collagen-binding site in the von Willebrand factor-A3 domain. *J Biol Chem* 2003;278:15035–15039.
3. Wu D, Vanhoorelbeke K, Cauwenberghs N, Meiring M, Depraetere H, Kotze HF, Deckmyn H. Inhibition of the von Willebrand (VWF)-collagen interaction by an antihuman VWF monoclonal antibody results in abolition of in vivo arterial platelet thrombus formation in baboons. *Blood* 2002;99:3623–3628.
4. Vanhoorelbeke K, Depraetere H, Romijn RA, Huizinga EG, De Maeyer M, Deckmyn H. A consensus tetra-peptide selected by phage display adopts the conformation of a dominant discontinuous epitope of a monoclonal anti-VWF antibody that inhibits the VWF-collagen interaction. *J Biol Chem* 2003;278:37815–37821.
5. Hellings M, De Maeyer M, Verheyden S, Hao Q, Van Damme EJM, Peumans WJ, Engelborghs Y. The dead-end elimination method, tryptophan rotamers, and fluorescence lifetimes. *Biophys J* 2003;85:1894–1902.
6. Sillen A, Díaz JF, Engelborghs Y. A step toward the prediction of the fluorescence lifetimes of tryptophan residues in proteins based on structural and spectral data. *Protein Science* 2000;9:158–169.
7. Bevington PR. Gradient-expansion algorithm. In *Data reduction and error analyses for the physical sciences*. New York: McGraw-Hill; 1969. p 235–240.
8. Beechem JM, Knutson JR, Ross JBA, Turner BW, Brand L. Global resolution of heterogeneous decay by phase modulation fluorometry: mixtures and proteins. *Biochemistry* 1983;22:6054–6058.

9. More JJ, Sorensen DC. Computing a trust region step. *SIAM J Sci Stat Comput* 1983;4:553–572.
10. Parker CA, Rees WT. Corrections of fluorescence spectra and the measurement of fluorescence quantum efficiency. *Analyst* 1960;85: 587–600.
11. Kirby EP, Steiner RFS. The influence of solvent and temperature upon the fluorescence of indole derivatives. *J Phys Chem* 1970;74: 4480–4490.
12. Sillen A, Engelborghs Y. The correct use of “average” fluorescence parameters. *Photochem Photobiol* 1998;67:475–486.
13. Weber G. Theory of differential phase fluorometry: detection of anisotropic molecular rotations. *J Phys Chem* 1977;66:4081–4091.
14. Lakowicz JR, Laczko G, Gryczinski I. 2-GHz frequency-domain fluorometer. *Rev Sci Instrum* 1985;57:2499–2506.
15. Lakowicz JR. *Principles of fluorescence spectroscopy*. New York: Kluwer Academic/Plenum Press; 1999. p 238–264.
16. De Maeyer M, Desmet J, Lasters I. The dead-end elimination theorem: mathematical aspects, implementation, optimizations, evaluation, and performance. *Methods Mol Biol* 2000;143:265–304.
17. De Maeyer M, Desmet J, Lasters I. All in one: a highly detailed rotamer library improves both the accuracy and speed in the modelling of sidechains by dead-end elimination. *Fold Des* 1997;2: 53–66.
18. Delhaise P, Bardiaux M, De Maeyer M, Prevost M, Vanbelle D, Donneux J, Lasters I, Vancustem E, Alard P, Wodak SJ. The BRUGEL package: toward computer-aided-design of macromolecules. *J Mol Graph* 1988;6:219–219.
19. Alard P, Wodak SJ. Detection of cavities in a set of interpenetrating spheres. *J Comp Chem* 1991;12:918–922.
20. Szabo AG, Rayner DM. Fluorescence decay of tryptophan conformers in aqueous solution. *J Am Chem Soc USA* 1980;102:554–563.